Layered Fibrotic Plaques Are the Predominant Component in Cardiac Allograft Vasculopathy Systematic Findings and Risk Stratification by OCT

Clemmensen, T.S.; Holm, N.R.; Eiskjaer, H.; Logstrup, B.B.; Christiansen, E.H.; Dijkstra, J.; ... ; Poulsen, S.H.

JACC: CARDIOVASCULAR IMAGING
VOL. 10, NO. 7, 2017

ISSN 1936-878X/$36.00
PUBLISHED BY ELSEVIER
http://dx.doi.org/10.1016/j.jcmg.2016.10.021

Layered Fibrotic Plaques Are the Predominant Component in Cardiac Allograft Vasculopathy

Systematic Findings and Risk Stratification by OCT

Tor Skibsted Clemmensen, MD,[a] Niels Ramsing Holm, MD,[a] Hans Eiskjær, MD, DMSc,[a] Brian Bridal Løgstrup, MD, PhD,[a] Evald Høj Christiansen, MD, PhD,[a] Jouke Dijkstra, PhD,[b] Trine Ørhøj Barkholt, MD,[a] Christian Juhl Terkelsen, MD, DMSc,[a] Michael Maeng, MD, PhD, DMSc,[a] Steen Hvitfeldt Poulsen, MD, DMSc[a]

ABSTRACT

OBJECTIVES The aims of this study were to characterize cardiac allograft vasculopathy (CAV) phenotypes using optical coherence tomography (OCT) and to evaluate the prognostic significance of OCT-determined CAV severity.

BACKGROUND Intravascular OCT enables in vivo characterization of CAV microstructure after heart transplantation.

METHODS Sixty-two patients undergoing heart transplantation were enrolled at routine angiography from September 2013 through October 2015 and prospectively followed until censoring on May 27, 2016. Optical coherence tomographic acquisitions aimed for the longest possible pull-backs, including proximal segments of all 3 major vessels. Plaques and bright spots were analyzed by delineating circumferential borders and measuring the angulation of total circumference. Layers were contoured for absolute and relative estimates. Nonfatal CAV progression (NFCP) during follow-up was registered. NFCP included occluded vessels or severe (≥70%) new angiographic coronary stenosis or percutaneous coronary intervention.

RESULTS A total of 172 vessels were categorized as follows: no CAV, n = 111; mild to moderate CAV (<70% stenosis), n = 40; and severe CAV (≥70% stenosis), n = 21. Layered fibrotic plaque (LFP) was the most prevalent plaque component, and the extent increased with angiographic CAV severity ($p < 0.01$). During follow-up, 22 of 172 vessels (13%) experienced NFCP. Median follow-up was 633 days (interquartile range: 432 to 808 days). The extent of LFP (hazard ratio: 5.0; 95% confidence interval: 2.1 to 12.4; $p < 0.0001$) and the extent of bright spots (hazard ratio: 6.2; 95% confidence interval: 2.4 to 15.8, $p < 0.001$) were strong predictors of NFCP. By combining LFP and bright spots, a strong NFCP predictive model was obtained (hazard ratio: 8.9; 95% confidence interval: 2.6 to 29.9; $p < 0.0001$).

CONCLUSIONS OCT enables the detection of CAV-associated plaque compositions and allows early detection and differentiation of vessel wall disease not visible on angiography. LFP was the most prevalent plaque component, was strongly associated with NFCP, and may be associated with stepwise CAV progression caused by organizing mural thrombi. (The GRAFT Study: Evaluation of Graft Function, Rejection and Cardiac Allograft Vasculopathy in First Heart Transplant Recipients; NCT02077764) (J Am Coll Cardiol Img 2017;10:773–84) © 2017 by the American College of Cardiology Foundation.

From the [a]Department of Cardiology, Aarhus University Hospital, Skejby, Denmark; and the [b]Division of Image Processing, Leiden University Medical Centre, Leiden, the Netherlands. Funding was received from the Health Research Fund of Central Denmark Region and the Danish Heart Association. The authors have reported that they have no relationships relevant to the contents of this paper to disclose.

Manuscript received July 14, 2016; revised manuscript received September 22, 2016, accepted October 20, 2016.

JACC: CARDIOVASCULAR IMAGING, VOL. 10, NO. 7, 2017
JULY 2017:773–84

ABBREVIATIONS AND ACRONYMS

CAV = cardiac allograft vasculopathy

CI = confidence interval

HTx = heart transplantation

ICC = intraclass correlation coefficient

IQR = interquartile range

IVUS = intravascular ultrasound

LAD = left anterior descending coronary artery

LFP = layered fibrotic plaque

NFCP = nonfatal cardiac allograft vasculopathy progression

OCT = optical coherence tomography

RCA = right coronary artery

Cardiac allograft vasculopathy (CAV) remains the most important long-term cardiac mortality cause after heart transplantation (HTx) (1). Autopsy studies describe CAV as a combination of atherosclerosis, concentric fibrotic intimal thickening, thrombosis, and inflammation (2,3). Most transplantation centers routinely perform coronary angiography to determine CAV severity and progression. However, conventional angiography often misses or underestimates the CAV burden. Hence, intravascular ultrasound (IVUS) diagnoses CAV in approximately 50% of HTx patients with normal results on angiography (4–8). IVUS is therefore widely used in HTx patients (9). In recent years, optical coherence tomography (OCT) has become the state-of-the-art high-resolution intravascular imaging modality for the assessment of coronary disease. IVUS and OCT detect CAV equally well when traditional IVUS parameters are used (10,11) (i.e., maximal intimal thickness and intima/media ratio). However, OCT provides 10-fold greater spatial resolution than IVUS and enables a more detailed evaluation of vessel wall microstructure. The use of OCT may therefore offer important, thus far undetectable in vivo insights into the nature and pathogenesis of CAV. If OCT enables differentiation among various vessel wall pathologies, it may be used for early detection of CAV and for CAV staging on the basis of coronary disease phenotypes.

SEE PAGE 785

In the present study, we characterized CAV phenotypes using OCT, evaluated the utility of OCT for CAV severity assessment, and determined the prognostic significance of CAV severity.

METHODS

PATIENTS. Patients undergoing routine angiography, right-heart catheterization, and echocardiography were included from September 6, 2013 through October 19, 2015. Patients ≥18 years of age with creatinine levels <200 μmol/l were included after providing informed written consent according to the principles of the Declaration of Helsinki. The Central Denmark Region Committees on Biomedical Research Ethics approved the study. The study was registered with ClinicalTrials.gov (NCT02077764).

Patients were prospectively followed from the time of OCT until death or censoring on May 27, 2016. Nonfatal CAV progression (NFCP) during follow-up was registered. NFCP included: 1) severe new coronary stenosis (≥70%) with or without percutaneous intervention; and 2) clinically suspected coronary spasm verified by angiography and/or electrocardiography. Patients who experienced NFCP were stratified at the time of their first NFCP episode.

CORONARY ANGIOGRAPHY AND OCT. Image acquisition. Coronary angiography was performed using a 6-F guiding catheter after administration of intracoronary nitroglycerin (200 μg) into the left main coronary artery and right coronary artery (RCA). At least 2 projections of each coronary artery were acquired.

Prior to OCT recordings, intravenous heparin 5,000 IU was administered. OCT was performed using Lunawave OCT (Terumo, Tokyo, Japan), aiming for the longest possible pull-backs and ensuring acquisition of proximal segments covering up to 150 mm of each major branch. Pull-back speed was adjusted to optimize the scan time to 3 to 4 s during flushing with 15 to 20 ml contrast. In case of inadequate image quality, the recordings were repeated after guiding catheter position adjustment. Recordings were obtained in the left main coronary artery, the left anterior descending coronary artery (LAD), the circumflex coronary artery, and the RCA.

Image analysis. ***Angiographic CAV assessment.*** All major branches with visual CAV were analyzed offline using 2-dimensional quantitative coronary analysis with QAngioXA 7.3 (Medis Medical Imaging, Leiden, the Netherlands). The reference vessel size and the maximal stenosis severity of each vessel were measured. Vessels were divided into 3 angiographic CAV groups by the severity of the stenosis according to guidelines from the International Society for Heart and Lung Transplantation (9): CAV 1 (mild), angiographic left main <50% or primary vessel or branch stenosis with a maximum lesion of <70%; CAV 2 (moderate), angiographic left main <50%, a single primary vessel ≥70%, or isolated branch stenosis ≥70% in branches of 2 systems; CAV 3 (severe), angiographic left main ≥50%, 2 or more primary vessels ≥70% stenosis, or isolated branch stenosis ≥70% in all 3 systems; or CAV 1 or CAV 2 with allograft dysfunction (defined as left ventricular ejection fraction <45%) or evidence of significant restrictive physiology (symptomatic patients with ratio of early to late ventricular filling velocities >2, isovolumetric relaxation time <60 ms, E-wave deceleration time <150 ms, right atrial pressure >12 mm Hg, pulmonary capillary wedge pressure >25 mm Hg, or cardiac index <2 l/min/m^2). Because

FIGURE 1 **Quantitative Optical Coherence Tomographic Vessel Layer and Plaque Analysis**

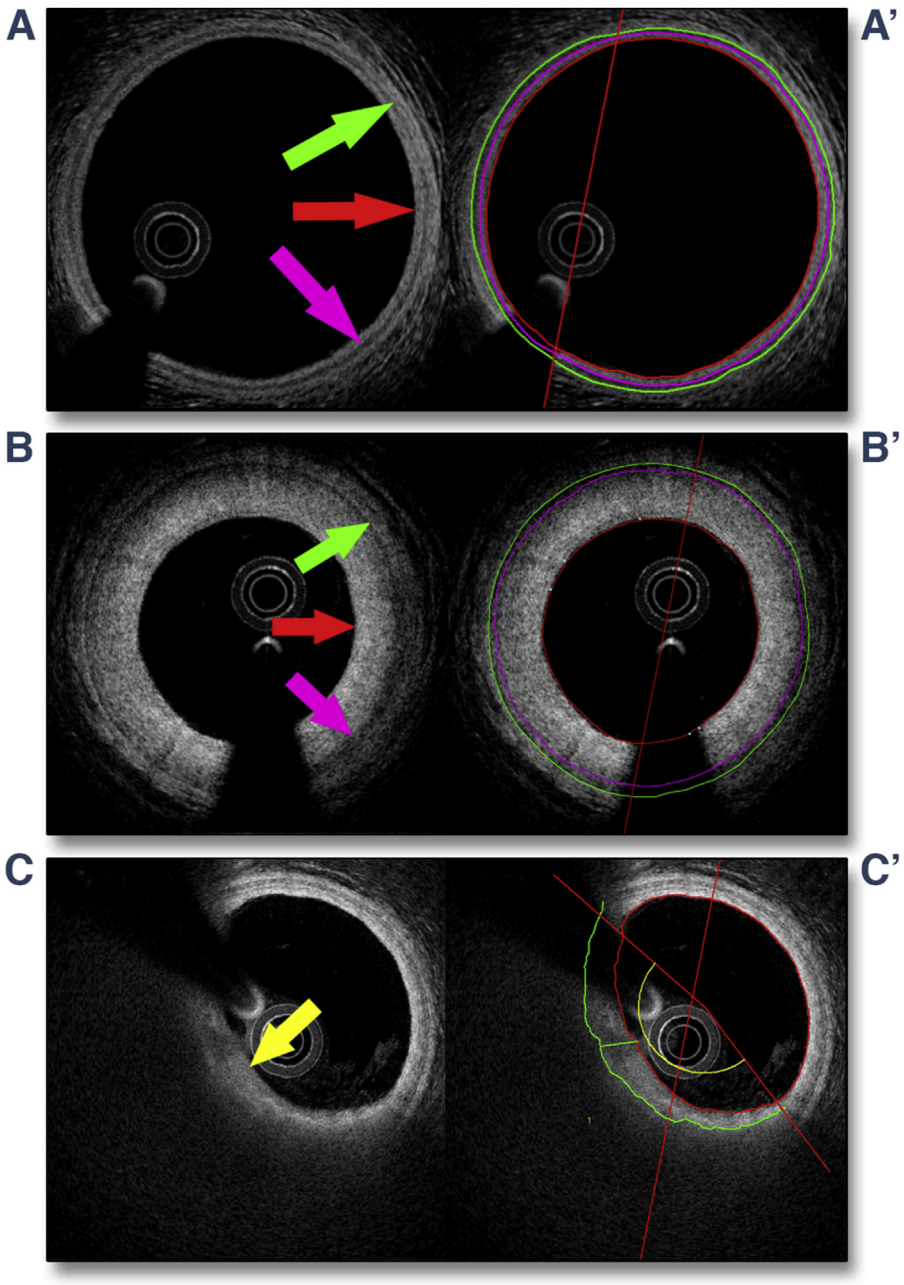

(A) Normal vessel; **(A′)** vessel layer analysis. **(B)** Intimal hypertrophy; **(B′)** vessel layer analysis. **(C)** Lipid plaque; **(C′)** lipid plaque with plaque analysis. **Green ring and arrow** indicate media-adventitia interface; **pink ring and arrow** denote intima-media interface; **red ring and arrow** denote luminal border; the **yellow ring and arrow** indicate plaque and plaque angle.

we could not discriminate between CAV 2 and CAV 3 in per-vessel analysis, we combined these groups. Furthermore, vessels with previous percutaneous intervention were classified as CAV 2 and 3 despite no present diameter stenosis ≥70%.

OCT analysis. Quantitative analysis was performed at 1-mm intervals using a customized version of the validated QCU-CMS analysis software (Medis Medical Imaging). Figure 1 shows quantitative OCT analysis. Vessel layer assessment included

JACC: CARDIOVASCULAR IMAGING, VOL. 10, NO. 7, 2017
JULY 2017:773–84

FIGURE 2 Range of Optical Coherence Tomographic Findings in the Heart Transplantation Study Population

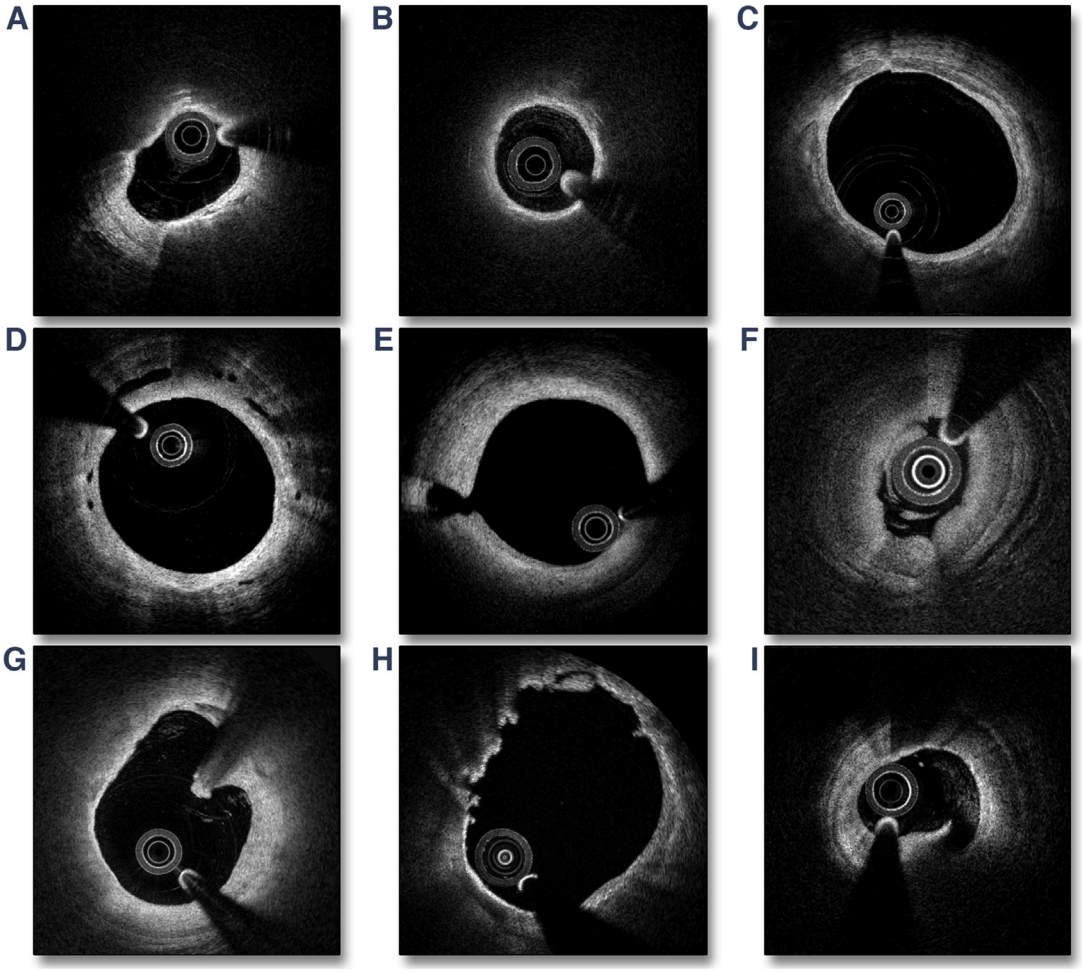

(A) Bright spots between 8 o'clock and 6 o'clock; **(B)** circumflex bright spots; **(C)** thin circumferential calcifications; **(D)** intimal microvessels; **(E)** side branch ostium with narrowing caused by fibrotic plaque formation; **(F)** coronary spasm identified by bulging intima and clamped side branch; **(G)** intraluminal thrombosis; **(H)** erosions and intraluminal thrombi; **(I)** plaque rupture.

measurements of luminal area, intimal area, and medial area. These parameters were obtained from 3 vessel contours: a lumen-intima interface contour, an intima-media interface contour, and a media-adventitia interface contour (**Figures 1A and 1B**). Plaque and bright-spot analysis was performed by delineating lateral plaque borders (**Figure 1C**), thereby measuring the angulation of circumferential plaque, and reporting the percentage of total circumference in analyzed frames. Plaques were classified as: 1) lipid (combined lipid pools and thin-cap fibroatheromas); 2) calcifications; or 3) layered fibrotic plaques (LFPs). The lipid plaques were defined as heterogenic, signal-poor, highly attenuating intimal regions with diffuse or poorly defined borders. Calcifications were defined as sharply delineated, heterogeneous, signal-poor regions. LFP was defined as homogeneous, signal-rich tissue but predominantly with a signal intensity lower than surrounding or deeper layers of intimal tissue and with a clearly layered structure. LFP could be identified as a separate plaque component superficial to other plaque types (lipid plaque, calcified plaque). Bright spots were defined as signal-rich attenuating regions within the intima layer and a signal intensity exceeding that of adjacent fibrotic tissue. Adaptions were based on Tearney et al. (12). **Figure 2** presents typical OCT findings in the analyzed HTx cohort.

The vessel layer contours were obtained in areas with no side branches and no atherosclerosis.

Qualitative analysis involved counting the number of side branches exceeding 1 mm and the number of intraluminal thromboses. Furthermore, the vessel disease phenotype was estimated and characterized as normal phenotype, thrombofibrotic phenotype, atherosclerotic phenotype only, and mixed atherosclerotic and thrombofibrotic phenotype. The thrombofibrotic phenotype was defined as 2 or more areas with LFP, bright spots without lipid plaque presence, or any combination of these. Atherosclerotic phenotype was defined as 1 or more areas with lipid plaques.

STATISTICAL METHODS. We analyzed data on a per-vessel level and a per-patient level. In patient-level analysis, we used the mean value from analyzed vessels for each variable.

Normally distributed data are presented as mean ± SD; non-normally distributed data are presented as median and (interquartile range [IQR]). Categorical data are presented as absolute values with percentages. Histograms and Q-Q plots were used to check continuous values for normality of the data distribution. Between-group differences were assessed by mixed-model analysis of variance. The intraclass correlation coefficient (ICC) was used to determine the correlation of OCT findings between the LAD, circumflex coronary artery, and RCA. Sensitivity and specificity were determined using receiver-operating characteristic curves. Optimal between-group cutoff points for plaque and vessel measurements were defined as the intersection points of sensitivity and specificity on the receiver-operating characteristic curves. Time-to-event data were evaluated using Kaplan-Meier estimates and Cox proportional hazards methods. Hazard ratios, 95% confidence intervals (CIs), and 2-sided p values were calculated using the Cox models. A p value <0.05 was considered to indicate statistical significance. Analyses were performed using Stata/IC 13 (StataCorp LP, College Station, Texas).

RESULTS

CLINICAL CHARACTERISTICS. We included 62 patients, of whom 31 had normal vessels by angiography (CAV 0), 17 had mild to moderate CAV by angiography (CAV 1), and 13 had severe CAV by angiography (CAV 2 and 3). No patients were reclassified as CAV 2 and 3 on the basis of International Society for Heart and Lung Transplantation graft dysfunction criteria. Table 1 presents the demographics of the angiographic CAV groups.

TABLE 1 Patient Characteristics According to Angiographic CAV Group

	CAV 0 (n = 31)	CAV 1 (n = 17)	CAV 2 and 3 (n = 13)	p Value*
Men	74	88	54	0.33
Age, yrs	53 ± 14	52 ± 9	56 ± 12	0.66
Donor age, yrs	40 ± 12	44 ± 14	46 ± 8	0.43
Time since transplantation, yrs	2.0 (1.0–7.0)	8.0 (1.1–11.0)	15.0 (11.0–16.0)	<0.001
Diabetes	13	24	8	0.45
Hypertension	90	82	92	0.64
Former PCI treatment	0	0	23	<0.001
Rejection score	7.0 (4.0–11.0)	10 (5.0–12.0)	10.0 (8.0–14.0)	0.08
Medication				
Prednisolone	58	47	15	<0.05
Ciclosporine	32	6	69	<0.001
Tacrolimus	68	94	31	<0.001
Everolimus	16	24	54	<0.05
Mycophenolate	90	75	46	<0.01
Statins	87	88	92	0.89
ACE/AT II inhibitor	77	75	69	0.86
Furosemide or bumetanide	19	6	23	0.42
Aspirin	26	63	100	<0.0001
Graft function				
Ejection fraction, %	64 ± 10	61 ± 8	59 ± 11	0.20
E/A ratio	2.0 ± 0.6	2.0 ± 1.0	2.1 ± 0.8	0.92
IVRT, ms	65 ± 15	66 ± 22	77 ± 30	0.22
E-wave deceleration time, ms	164 ± 38	163 ± 43	151 ± 56	0.64
Right atrial pressure, mm Hg	4.1 ± 2.4	4.5 ± 4.0	5.9 ± 3.3	0.21
PCWP, mm Hg	10.5 ± 4.4	10.4 ± 5.0	10.6 ± 5.9	0.99
Cardiac index, l/min/m^2	2.9 ± 0.5	2.6 ± 0.4	2.7 ± 0.3	0.09
Biochemistry				
Creatinine, μmol/l	99 (80–120)	100 (82–116)	120 (80–124)	0.64
Hemoglobin, mmol/l	8.7 (7.6–9.0)	8.4 (7.7–9.3)	8.5 (8.1–9.0)	0.61
Total cholesterol, mmol/l	4.5 (3.7–5.4)	4.7 (4.0–4.9)	5.1 (4.5–6.2)	0.26
Troponin T, ng/l	13 (5–18)	8 (5–17)	14 (5–26)	0.35
NT-proBNP, ng/l	335 (180–678)	249 (137–486)	1203 (397–1,631)	<0.05

Values are %, mean ± SD, or median (interquartile range). *Testing difference between the 3 groups.

ACE = angiotensin-converting enzyme; AT II = angiotensin II; CAV = cardiac allograft vasculopathy; E/A ratio = ratio of early to late ventricular filling velocities; IVRT = isovolumetric relaxation time; NT-proBNP = N-terminal pro–B-type natriuretic peptide; PCI = percutaneous coronary intervention; PCWP = pulmonary capillary wedge pressure.

FEASIBILITY OF OCT. In 1 of the 62 patients we were unable to obtain analyzable images from any of the vessels. The analysis included 59 LAD vessels (95%), 56 circumflex vessels (90%), and 57 RCA vessels (91%). A total of 11,158 frames from 172 vessels were analyzed. No patients had complications due to angiography or acquisition of OCT.

ANGIOGRAPHIC VESSEL ANALYSIS. The mean length of the analyzed vessels did not differ between angiographic CAV groups (CAV 1, 80 ± 20 mm; CAV 2 and 3, 74 ± 21 mm; p = 0.14). Median maximal stenosis in the CAV groups was 35% (IQR: 30% to 43%)

TABLE 2 Qualitative OCT Analysis, Stratified According to Angiographic CAV Groups

	CAV 0	CAV 1	CAV 2 and 3	p Value*
Patient level	n = 31	n = 17	n = 13	
Number of side branches >1 mm	7.5 ± 0.3	7.2 ± 0.4	4.9 ± 0.4	<0.0001
OCT quality†	4.3 ± 0.1	4.5 ± 0.1	4.4 ± 0.1	0.35
Number of intraluminal thrombi	0.02 ± 0.2	0.12 ± 0.2	1.34 ± 0.2	<0.0001
Number of erosions	0	0.08 ± 0.1	0.68 ± 0.1	<0.0001
Vessel level	n = 111	n = 40	n = 21	
Number of side branches >1 mm	7.5 ± 0.2	6.1 ± 0.4	4.8 ± 0.5	<0.0001
OCT quality†	4.3 ± 0.1	4.5 ± 0.1	4.6 ± 0.2	0.14
Number of intraluminal thrombi	0.1 ± 0.1	0.3 ± 0.2	2.0 ± 0.3	<0.0001
Number of erosions	0.04 ± 0.1	0.28 ± 0.1	0.65 ± 0.1	<0.0001
Phenotype				
Normal	47	3	0	<0.0001
Thrombofibrotic	32	50	52	0.06
Atherosclerotic	10	10	10	0.99
Mixed thrombofibrotic and atherosclerotic	11	38	38	<0.001

Values are mixed model coefficient ± SE or %. *Testing difference between the 3 groups. †On a scale ranging from 1 (unreadable OCT images) to 5 (optimal image quality).

CAV = cardiac allograft vasculopathy; OCT = optical coherence tomography.

(CAV 1) and 76% (IQR: 71% to 83%) (CAV 2 and 3) ($p < 0.0001$).

CLINICAL FOLLOW-UP. Median time from OCT assessment to clinical follow-up was 605 days (IQR: 373 to 759 days). NFCP occurred in 13% of vessels (22 of 172) and 20% of patients (12 of 61) during follow-up. One vessel was censored because of acute myocardial infarction. Twenty-one vessels were censored because of severe stenosis. The majority of censored vessels had angiographic CAV. Hence, 2 vessels were classified as CAV 0, 10 vessels as CAV 1, and 10 vessels as CAV 2 and 3. Percutaneous coronary intervention was performed in 13 vessels. Likewise, the majority of censored patients had angiographic CAV; 1 patient had CAV 0, 2 patients CAV 1, and 9 patients had CAV 2 and 3.

QUALITATIVE OCT ANALYSIS: PATIENT LEVEL. Table 2 displays the qualitative OCT results on the patient level. The number of side branches exceeding 1 mm in diameter decreased significantly, whereas the number of fresh luminal thrombi and erosions increased significantly with increasing angiographic CAV severity ($p < 0.0001$).

QUALITATIVE OCT ANALYSIS: VESSEL LEVEL. Table 2 displays the qualitative OCT results on the vessel level. Fresh luminal thrombi or plaque ruptures were observed in 7 CAV 0 vessels (6%), 9 CAV 1 vessels (23%), and 9 CAV 2 and 3 vessels (38%) ($p < 0.0001$).

The OCT-established qualitative phenotypes in mild to moderate CAV and in the severe CAV groups were comparable, with the majority of vessels showing the thrombofibrotic phenotype (50% and 52%) or a mix of the thrombofibrotic and atherosclerotic phenotypes (38% and 38%). Importantly, 53% of vessels with no angiographic CAV had abnormal phenotype by OCT, with thrombofibrotic phenotype being the most prevalent (32%). We found that vessels with the thrombofibrotic phenotype ($p < 0.001$) or a mix of thrombofibrotic and atherosclerotic phenotypes ($p < 0.001$) had greater NFCP risk during follow-up than vessels with normal phenotype. Furthermore, 20 of 22 NFCP episodes were seen in vessels with either thrombofibrotic or a mix of thrombofibrotic and atherosclerotic phenotypes.

QUANTITATIVE PLAQUE ANALYSIS BY OCT: PATIENT LEVEL. Table 3 shows the quantitative plaque results on the patient level. All OCT-detected plaque categories increased with the severity of angiographic CAV. However, no difference was seen in LFP between CAV 1 and CAV 2 and 3 vessels ($p = 0.88$).

QUANTITATIVE PLAQUE ANALYSIS BY OCT: VESSEL LEVEL. Table 3 presents the quantitative plaque results on the vessel level. Furthermore, Figure 3A shows the plaque distribution in the 3 CAV vessel groups. For all plaque categories, the extent of plaque assessed by OCT increased with the severity of angiographic CAV. However, no difference was found between CAV 0 vessels and CAV 1 vessels regarding the extent of LFP ($p = 0.55$), bright spots ($p = 0.90$), and calcifications ($p = 0.20$). In contrast, CAV 2 and 3 vessels had a significantly higher lipid plaque extent than CAV 1 vessels ($p < 0.0001$). We found a strong NFCP predictive ability for the extent of calcifications, bright spots, and LFP (Figure 3B). Interestingly, LFPs were the most prevalent plaque component. These plaques were seen on the surface of lipid plaques and calcified plaques, but they were more prevalent in segments with no other advanced plaques (Figure 4). By combining the extent of LFP (cutoff 9.6%) and bright spots (cutoff 7.9%), we obtained a strong NFCP predictive model (hazard ratio: 8.9; 95% CI: 2.6 to 29.9; $p < 0.0001$). Bright spots ≥7.9% or LFP ≥9.6% was seen in 77 vessels. The remaining 95 vessels had <5.5% bright spots and <8.8% LFP. The vessels with increased NFCP risk consisted of 31 CAV 0 vessels, 28 CAV 1 vessels, and 18 CAV 2 and 3 vessels. The risk-stratified vessels were applied at the patient level. Patients who were at increased NFCP risk included 15 patients with no angiographic CAV (48% of CAV 0 patients), 10 patients with mild to moderate CAV (59% of CAV 1 patients), and 13 patients with severe CAV (100% of CAV 2 and 3 patients).

QUANTITATIVE VESSEL LAYER THICKNESS ANALYSIS BY OCT: PATIENT LEVEL. The quantitative vessel layer analysis on the patient level is shown in Table 3. No difference in minimal luminal area was observed between the groups. In contrast, lumen/intima ratio, intima/media ratio, and intimal area were significantly altered with increasing angiographic CAV severity.

QUANTITATIVE VESSEL LAYER THICKNESS ANALYSIS BY OCT: VESSEL LEVEL. The results of quantitative vessel layer analysis are shown in Table 3. Minimal luminal area was significantly lower in the CAV 2 and 3 vessels than in the CAV 0 and CAV 1 vessels. No difference in minimal luminal area was seen between CAV 0 and CAV 1 vessels (p = 0.22). Likewise, no between-group differences were observed regarding media layer area. In contrast, intima layer area increased significantly with the severity of angiographic CAV. Additionally, intima/media ratio increased with the severity of angiographic CAV. Furthermore, lumen/intima ratio decreased with the severity of angiographic CAV. We found a strong correlation between NFCP and intimal thickness. Subsequently, intima/media ratio and lumen/intima ratio also predicted NFCP (Figure 5B).

PREDICTION OF NFCP BY QUANTITATIVE OCT. Table 4 show the NFCP predictive ability of quantitative OCT parameters on the per-patient and per-vessel levels. In the unadjusted analysis, calcifications, LFP, bright spots, intimal area, intima/media ratio, and lumen/intima ratio all predicted NFCP on both the per-patient and per-vessel levels. After adjustment of time since HTx and angiographic CAV class, LFP showed borderline significant NFCP predictive value (p = 0.06). Intimal area, lumen/intima ratio, and intima/media ratio continued to show significant NFCP predictive value after adjustment.

INTRAOBSERVER AND INTEROBSERVER VARIATION AND THE CORRELATION BETWEEN MAJOR CORONARY VESSELS. In comparison of the 3 vessels, ICC analysis showed a moderate correlation between the extent of lipid plaques (ICC = 0.84; 95% CI: 0.77 to 0.89), LFP (ICC = 0.74; 95% CI: 0.63 to 0.82), and bright spot distribution (ICC = 0.83; 95% CI: 0.76 to 0.89). A good correlation was seen comparing lumen/intima ratio between the 3 major vessels (ICC = 0.84; 95% CI: 0.77 to 0.90). Finally, a moderate correlation was seen between the intima/media ratio when the 3 major vessels were compared (ICC = 0.69; 95% CI: 0.56 to 0.79).

Intraobserver and interobserver variation was based on the analysis of 378 frames from 5 patients. The results are presented in Table 5. Despite the small sample, ICCs for both plaque and vessel wall measurements seemed sound, even though some variation was noted in the plaque analysis.

TABLE 3 Quantitative OCT Analysis, Stratified According to Angiographic CAV Groups

	CAV 0	CAV 1	CAV 2 and 3	p Value*
Patient level	n = 31	n = 17	n = 13	
Length, mm	75 ± 2	79 ± 3	69 ± 4	0.16
Plaque analysis, frame level				
Lipid pools, %†	1.7 ± 1.4	4.8 ± 2.0	15.9 ± 2.2	<0.0001
Calcifications, %†	0.3 ± 0.5	2.0 ± 0.7	3.7 ± 0.8	<0.01
Layered fibrotic plaque, %†	3.3 ± 1.9	15.6 ± 2.5	15.0 ± 2.9	<0.0001
Bright spots, %†	2.9 ± 2.1	7.6 ± 3.0	29.3 ± 3.3	<0.0001
Areas				
Luminal area, minimal, mm^2	5.3 ± 0.3	4.0 ± 0.5	4.2 ± 0.5	<0.05
Luminal area, mean, mm^2	9.3 ± 0.4	7.9 ± 0.5	8.6 ± 0.6	0.11
Intimal area, maximal, mm^2	3.9 ± 0.4	5.7 ± 0.5	7.7 ± 0.6	<0.0001
Intimal area, mean, mm^2	1.8 ± 0.3	2.8 ± 0.4	4.9 ± 0.4	<0.0001
Medial area, mean, mm^2	1.0 ± 0.1	1.1 ± 0.1	1.2 ± 0.1	0.21
Ratios				
Lumen/intima, mean	6.1 ± 0.3	3.9 ± 0.4	2.3 ± 0.4	<0.0001
Intima/media, mean	1.7 ± 0.1	2.5 ± 0.2	4.0 ± 0.2	<0.0001
Vessel level	n = 111	n = 40	n = 21	
Length, mm	77 ± 2	75 ± 4	68 ± 5	0.29
Plaque analysis, frame level				
Lipid pools, %†	4.3 ± 1.2	5.8 ± 1.3	11.8 ± 1.7	<0.0001
Calcifications, %†	1.1 ± 0.4	2.0 ± 0.5	2.6 ± 0.6	<0.05
Layered fibrotic plaque, %†	7.2 ± 1.6	12.4 ± 1.9	13.9 ± 2.6	<0.01
Bright spots, %†	8.5 ± 2.0	12.4 ± 2.3	12.1 ± 2.9	0.11
Areas				
Luminal area, minimal, mm^2	5.0 ± 0.3	4.4 ± 0.4	3.2 ± 0.6	<0.05
Luminal area, mean, mm^2	9.0 ± 0.3	8.4 ± 0.5	7.9 ± 0.7	0.25
Intimal area, maximal, mm^2	4.6 ± 0.3	5.9 ± 0.4	6.9 ± 0.6	<0.001
Intimal area, mean, mm^2	2.1 ± 0.2	3.3 ± 0.3	4.6 ± 0.4	<0.0001
Medial area, mean, mm^2	1.1 ± 0.0	1.1 ± 0.1	1.2 ± 0.1	0.40
Ratios				
Lumen/intima, mean	5.1 ± 0.3	4.3 ± 0.3	3.3 ± 0.4	<0.0001
Intima/media, mean	1.8 ± 0.1	2.9 ± 0.2	4.0 ± 0.2	<0.0001

Values are mixed model coefficient ± SE. *Testing difference between the 3 groups. †Mean percentage of circumference angle.

CAV = cardiac allograft vasculopathy.

DISCUSSION

We describe a comprehensive OCT evaluation of all 3 major coronary arteries in HTx patients. We found that angiographic CAV was a manifestation of 3 main components: regular atherosclerotic plaques, LFP, and bright spots. Using OCT, we were able to reclassify the population of HTx patients according to vessel and plaque components. OCT showed that 66% of HTx patients had a high degree of adverse vessel wall components, which is clearly associated with

FIGURE 3 Variation in Optical Coherence Tomography–Detected Plaque Components Between CAV Groups on a Per-Vessel Level

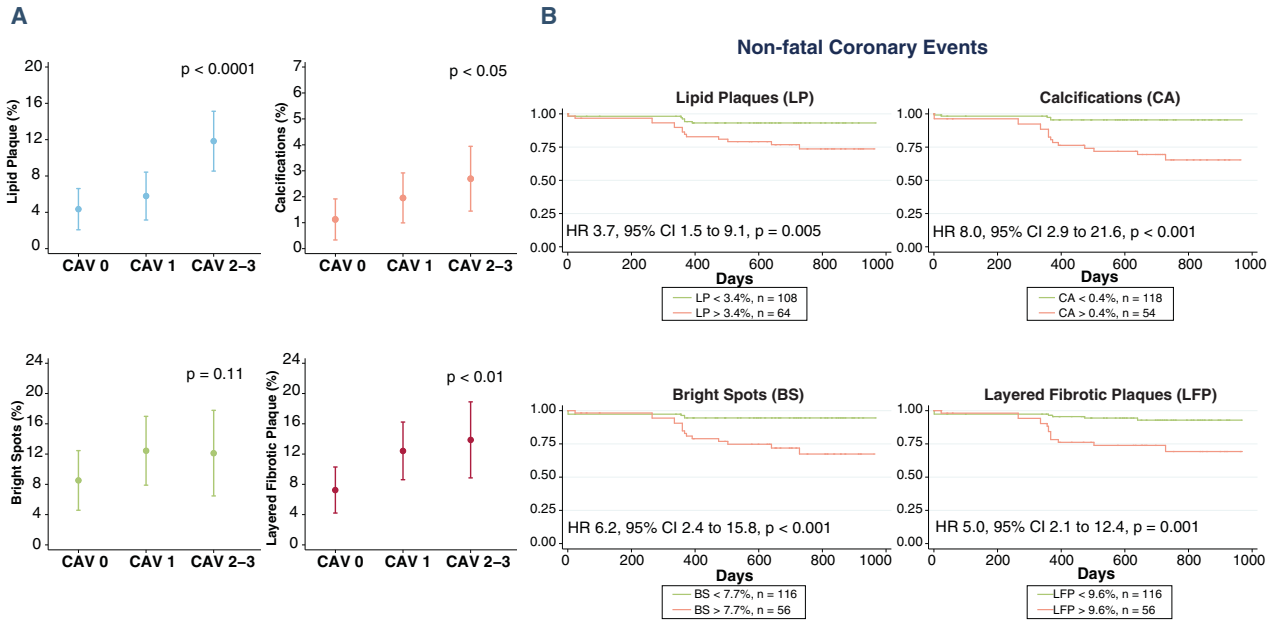

(A) Margin plots with 95% confidence interval (CI) demonstrating difference between cardiac allograft vasculopathy (CAV) groups regarding lipid plaques (LP), calcifications (CA), bright spots (BS), and layered fibrotic plaques (LFP). **(B)** Kaplan-Meier curves and hazard ratios (HRs) for the prognostic value of the plaque components.

increased NFCP risk. LFP and bright spots were the quantitatively most important plaque components in graft vasculopathy and were strongly associated with NFCP. Asymptomatic plaque rupture and intraluminal thrombi were also observed.

The ability to detect plaque morphology in vivo seems essential for HTx patients because their coronary disease is often different from traditional atherosclerotic coronary heart disease. Though promising, OCT has been used in only a few small 1-vessel HTx studies (10,11,13-15). Cassar et al. (13) performed a comprehensive OCT plaque evaluation in the proximal 30 mm of 53 LADs. Interestingly, they found a high prevalence of lipid pools and complex layered plaques. The investigators concluded that the latter may represent repeated thrombosis, which could be a possible underlying mechanism of CAV. These findings are of great importance because they challenge the traditional view that CAV is a disease characterized by concentric fibrotic intima thickening. In our study, the most exceptional feature of the coronary vessel wall microstructure was the high prevalence of LFP and bright spots. Bright spots are known to represent macrophages (16), and in HTx patients they may indicate chronic vascular rejection. An abundance of LFP could suggest the presence of organized and repeated mural arterial thrombosis. The layered appearance with slightly lower signal intensity of superficial fibrotic layers suggests a relatively young mural thrombus age. With time, the mural thrombus may progress to a more organized fibrotic stage leading to a more homogeneous intimal appearance. This is noteworthy because intravascular thrombosis in HTx vessels may be the cause of intimal fibrotic thickness, loss of side branches, reduced coronary perfusion, and eventually graft dysfunction and death.

The pathogenesis of mural coronary thrombus formation in HTx patients remains largely unknown. Autopsy and IVUS-virtual histology studies of HTx patients have previously shown a high prevalence of nonocclusive thrombi (3,17). These thrombi were layered on discontinuous or absent endothelium without atheromatous lesions (3). Similarly, in our study LFPs were observed both with and without communication to lipid plaques and calcifications. Hence, underlying plaque erosion may lead to thrombus formation in some vessels, and local vessel wall inflammation, here visualized as bright spots, may be part of this process. However, the underlying tissue has a normal appearance in many vessels.

FIGURE 4 Morphology of Layered Fibrotic Plaques

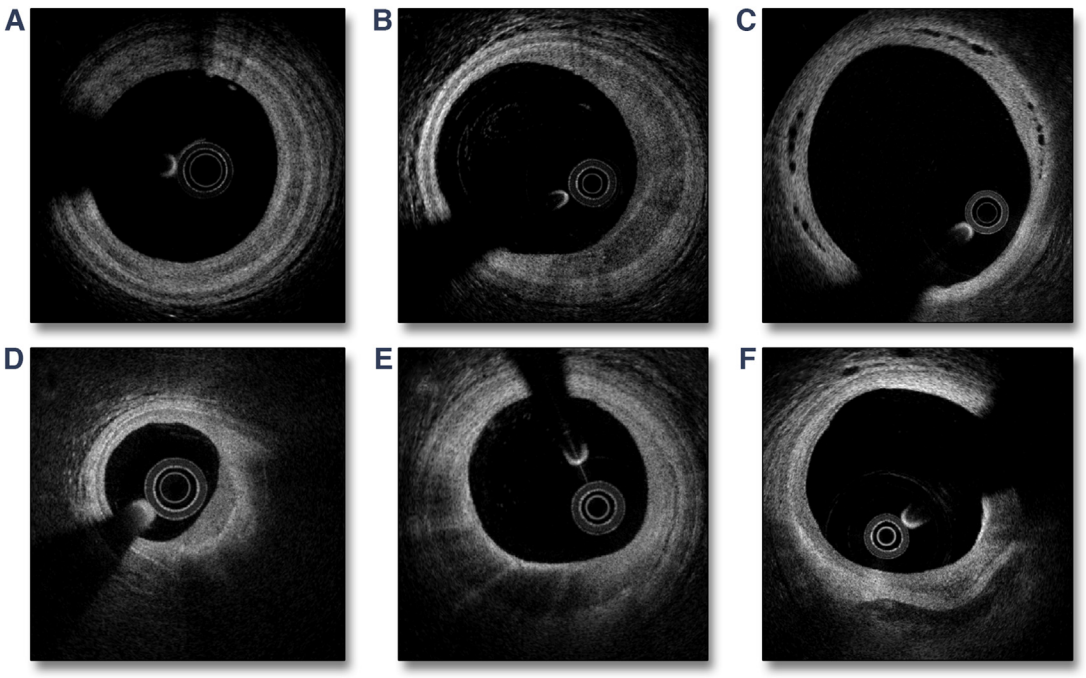

(A) Circumflex-layered fibrotic plaque; **(B)** crescent-shaped layered fibrotic plaque; **(C)** microvasculature in the interface between the native intima layer and the added layer of fibrotic tissue; **(D)** layered fibrotic plaque on the surface of lipid plaque; **(E)** bright spots on the luminal surface of layered fibrotic plaque; **(F)** layered fibrotic plaque on the surface of calcified plaque.

Thrombus formation could therefore be triggered by luminal factors but also by dysfunctional endothelium due to inflammation at the graft-recipient interface. Platelets are the cellular mediators of thrombosis, but they also play an important role in vascular inflammation (18). In our study, the number of intraluminal thrombi increased with CAV severity. Platelets may therefore have an important role in the development of CAV and coronary thrombi in HTx patients (19). It has been proposed that hypercoagulability and endothelial dysfunction may be involved in a murine aortic allograft model in which clopidogrel significantly decreased intimal proliferation (20). Likewise, aspirin in combination with simvastatin significantly reduced vascular damage and increased survival in a rat HTx model (21). Future studies should address whether CAV progression in HTx patients with early identification of LFP can be reduced by antiplatelet therapy and anticoagulation therapy.

Our study shows that the phenotypes vary significantly in HTx coronary vessel disease. Furthermore, the correlation of OCT parameters between the 3 major vessels showed noteworthy variation. A comprehensive OCT evaluation of CAV should therefore involve assessment of all 3 major coronary arteries. The average contrast use for 3-vessel OCT was 70 to 90 ml, and the additional procedure time for OCT was about 10 to 20 min. In our study, no patients experienced clinically meaningful renal function deterioration after OCT. However, additional contrast use must be carefully considered in HTx patients with more advanced renal dysfunction than the patients in this study. In contrast to OCT, IVUS can be performed with minimal contrast use. CAV screening by IVUS has prognostic value both in the early (<1 year) (5) and late (>1 year) (4,22) phases after HTx. Similarly, our study reveals great NFCP predictive value of vessel wall assessment. The main advantage of OCT compared with IVUS is the ability to perform in vivo plaque analysis with microstructure characterization. Our plaque analysis revealed a high extent of bright spots and LFP, and the combination of these components was strongly associated with NFCP. Therefore, this assessment may be used for risk stratification and may guide medical therapy. However, before OCT is recommended as an essential part of CAV surveillance, future larger studies should evaluate if OCT-based CAV assessment provides

FIGURE 5 Variation in Optical Coherence Tomography-Detected Vessel Layer Parameters Between CAV Groups on a Per-Vessel Level

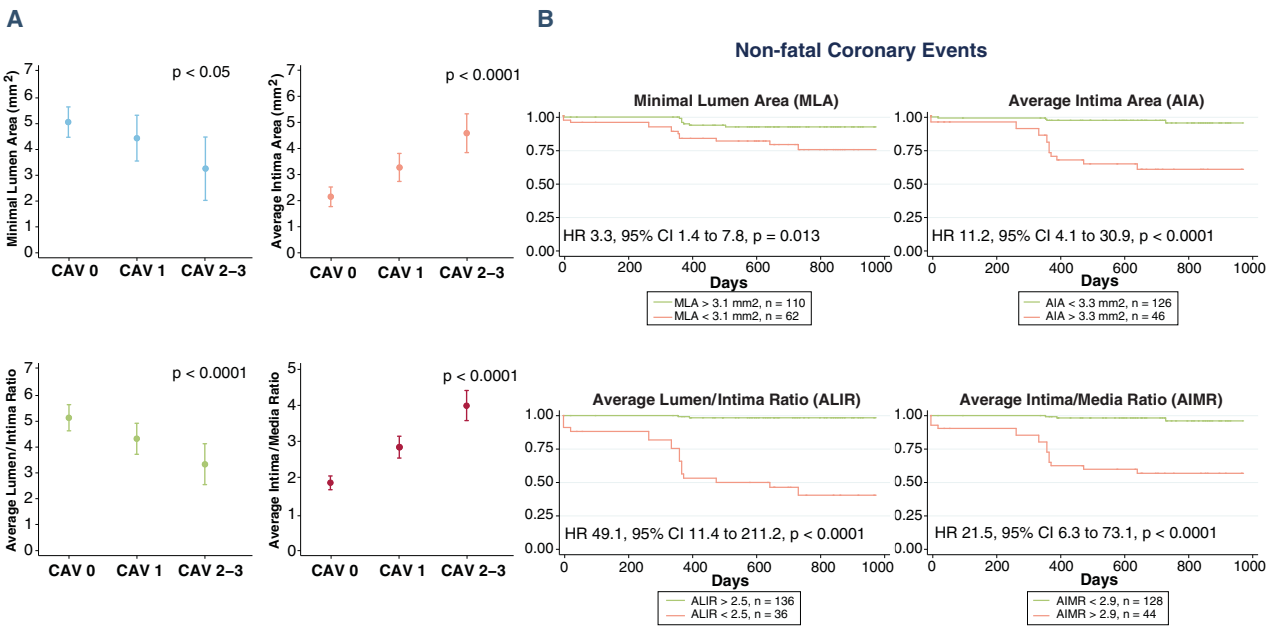

(A) Margins plot with 95% confidence interval (CI) demonstrating difference between cardiac allograft vasculopathy (CAV) groups regarding minimal luminal area (MLA), average intima area (AIA), average lumen/intima ratio (ALIR), and average intima/media ratio (AIMR). **(B)** Kaplan-Meier curves and hazard ratios (HRs) for the prognostic value of the vessels layer parameters.

TABLE 4 Nonfatal Cardiac Allograft Vasculopathy Progression Predictive Ability by Optical Coherence Tomographic Parameters

	Cutoff	AUC	Sensitivity	Specificity	Unadjusted Hazard Ratio (95% CI)	Adjusted Hazard Ratio* (95% CI)
Patient level						
Lipid plaque	3.6%	0.79	75%	76%	6.5 (1.8-24.1)‡	
Calcifications	0.4%	0.77	75%	71%	3.8 (1.2-12.8)†	
Layered fibrotic plaque	9.9%	0.82	67%	76%	3.8 (1.2-12.0)†	
Bright spots	7.1%	0.84	75%	76%	7.0 (1.9-26.1)‡	
Luminal area, minimal	4.0 mm^2	0.63	67%	57%	1.0 (0.3-3.0)	
Intimal area, mean	2.7 mm^2	0.83	75%	76%	9.0 (2.4-33.4)§	
Lumen/intima, mean	3.0 mm^2/mm^2	0.90	83%	84%	10.1 (2.7-37.3)§	
Intima/media, mean	2.6 mm^2/mm^2	0.88	83%	84%	17.1 (3.7-78.5)‖	
Vessel level						
Lipid plaque	3.4%	0.74	68%	67%	3.7 (1.5-9.1)‡	1.2 (0.5-3.3)
Calcifications	0.4%	0.79	77%	75%	8.0 (2.9-21.6)‖	2.5 (0.8-7.1)
Layered fibrotic plaque	9.6%	0.80	73%	73%	5.0 (2.1-12.4)‖	2.5 (1.0-6.1)
Bright spots	7.9%	0.82	73%	73%	6.2 (2.4-15.8)‖	1.7 (0.6-4.8)
Luminal area, minimal	3.1 mm^2	0.70	68%	68%	3.3 (1.4-7.8)†	1.9 (0.8-4.6)
Intimal area, mean	3.3 mm^2	0.89	86%	81%	11.2 (4.1-30.9)‖	3.8 (1.3-11.3)†
Lumen/intima, mean	2.5 mm^2/mm^2	0.95	90%	90%	49.1 (11.4-211.2)‖	19.5 (3.9-98.0)‖
Intima/media, mean	2.9 mm^2/mm^2	0.92	86%	84%	21.5 (6.3-73.1)‖	6.9 (1.7-27.9)‡

*Adjusted for time since heart transplantation and angiographic cardiac allograft vasculopathy class. †$p < 0.05$. ‡$p < 0.01$. §$p < 0.001$. ‖$p < 0.0001$.
AUC = area under the curve; CI = confidence interval.

TABLE 5 Intraobserver and Interobserver Variation

	Intraobserver Variation			Interobserver Variation		
	ICC (95% CI)	CV	Difference	ICC (95% CI)	CV	Difference
Plaque analysis						
Calcifications	1.00 (0.99-1.00)	9.5%	0.04 ± 0.6	0.99 (0.96-1.00)	17%	0.6 ± 1.0
Lipid plaques	0.98 (0.89-1.00)	44%	0.4 ± 0.8	1.00 (0.98-1.00)	17%	0.2 ± 0.4
Bright spots	0.97 (0.85-0.99)	31%	1.2 ± 2.6	0.85 (0.46-0.97)	41%	1.3 ± 3.1
Layered fibrotic plaque	0.99 (0.95-1.00)	12%	1.6 ± 3.4	0.98 (0.88-1.00)	23%	4.0 ± 5.7
Vessel layer analysis						
Luminal area, minimum	1.00 (1.00-1.00)	0.5%	0.002 ± 0.03	1.00 (1.00-1.00)	2.9%	0.17 ± 0.19
Intimal area, mean	1.00 (1.00-1.00)	0.7%	0.005 ± 0.03	1.00 (1.00-1.00)	1.7%	0.10 ± 0.07
Lumen/intima, mean	1.00 (1.00-1.00)	1.3%	0.04 ± 0.05	0.99 (0.97-1.00)	6.6%	0.25 ± 0.28
Intima/media, mean	0.99 (0.91-1.00)	3.9%	0.07 ± 0.11	0.98 (0.87-1.00)	8.7%	0.46 ± 0.20

CI = confidence interval; CV = coefficient of variation; ICC = intraclass correlation coefficient.

prognostic value beyond the standard angiographic assessment.

STUDY LIMITATIONS. This study was a single-center experience in a small cohort of patients. Only 12 patients experienced NFCP. Therefore, we were unable to perform multivariable analysis on the patient level. Furthermore, we do not have histological confirmation of our findings. However, patients were extensively studied using multivessel imaging, and autopsy studies have previously demonstrated findings similar to ours with a high prevalence of coronary mural thrombosis in HTx patients.

The interobserver and intraobserver analysis was based on a large number of frames from 5 randomly selected patients. Thus, it was likely to be influenced by the particular patients selected, and a larger sample size is warranted to determine more reliable coefficients of variation and ICCs for the OCT parameters.

CONCLUSIONS

OCT provided incremental value to traditional angiography by adding information about plaque morphology and vessel wall structure. LFP was the most prevalent plaque component and was found to be strongly associated with NFCP. The detection of LFP and bright spots by OCT was identified as a significant prognostic marker for the prediction of NFCP.

ACKNOWLEDGMENTS The authors thank the nurses and physicians at the coronary catheterization laboratory for their assistance during optical coherence tomographic acquisition.

ADDRESS FOR CORRESPONDENCE: Dr. Tor Skibsted Clemmensen, Department of Cardiology, Aarhus University Hospital Skejby, Palle Juul-Jensens Boulevard 99, 8200 Aarhus N, Denmark. E-mail: torclemm@rm.dk.

PERSPECTIVES

COMPETENCY IN MEDICAL KNOWLEDGE: OCT enables in vivo characterization of CAV microstructure after HTx and may be used for risk stratification. We found that CAV is a manifestation of 3 main components: regular atherosclerotic plaques, LFPs, and bright spots. LFP is the most prevalent plaque component, is strongly related to CAV progression during follow-up, and may be associated with stepwise progression of organized mural thrombi.

TRANSLATIONAL OUTLOOK: Future larger studies should validate and test if OCT-based CAV assessment provides prognostic value beyond the standard angiographic assessment. Furthermore, additional studies should address whether CAV progression in HTx patients with early identification of LFPs can be reduced by antiplatelet therapy and anticoagulation therapy.

REFERENCES

1. Stehlik J, Edwards LB, Kucheryavaya AY, et al. The Registry of the International Society for Heart and Lung Transplantation: 29th official adult heart transplant report—2012. J Heart Lung Transplant 2012;31:1052–64.

2. Lu WH, Palatnik K, Fishbein GA, et al. Diverse morphologic manifestations of cardiac allograft vasculopathy: a pathologic study of 64 allograft hearts. J Heart Lung Transplant 2011;30:1044–50.

3. Arbustini E, Dal Bello B, Morbini P, Gavazzi A, Specchia G, Vigano M. Multiple coronary thrombosis and allograft vascular disease. Transplant Proc 1998;30:1922–4.

4. Kobashigawa JA, Tobis JM, Starling RC, et al. Multicenter intravascular ultrasound validation study among heart transplant recipients: outcomes after five years. J Am Coll Cardiol 2005;45:1532–7.

5. Tuzcu EM, Kapadia SR, Sachar R, et al. Intravascular ultrasound evidence of angiographically silent progression in coronary atherosclerosis

predicts long-term morbidity and mortality after cardiac transplantation. J Am Coll Cardiol 2005; 45:1538–42.

6. Tona F, Osto E, Tarantini G, et al. Coronary flow reserve by transthoracic echocardiography predicts epicardial intimal thickening in cardiac allograft vasculopathy. Am J Transplant 2010;10: 1668–76.

7. Kass M, Allan R, Haddad H. Diagnosis of graft coronary artery disease. Curr Opin Cardiol 2007; 22:139–45.

8. Pollack A, Nazif T, Mancini D, Weisz G. Detection and imaging of cardiac allograft vasculopathy. J Am Coll Cardiol Img 2013;6:613–23.

9. Mehra MR, Crespo-Leiro MG, Dipchand A, et al. International Society for Heart and Lung Transplantation working formulation of a standardized nomenclature for cardiac allograft vasculopathy—2010. J Heart Lung Transplant 2010;29:717–27.

10. Khandhar SJ, Yamamoto H, Teuteberg JJ, et al. Optical coherence tomography for characterization of cardiac allograft vasculopathy after heart transplantation (OCTCAV study). J Heart Lung Transplant 2013;32:596–602.

11. Garrido IP, Garcia-Lara J, Pinar E, et al. Optical coherence tomography and highly sensitivity troponin T for evaluating cardiac allograft vasculopathy. Am J Cardiol 2012;110:655–61.

12. Tearney GJ, Regar E, Akasaka T, et al. Consensus standards for acquisition, measurement, and reporting of intravascular optical coherence tomography studies: a report from the International Working Group for Intravascular Optical Coherence Tomography Standardization and Validation. J Am Coll Cardiol 2012;59: 1058–72.

13. Cassar A, Matsuo Y, Herrmann J, et al. Coronary atherosclerosis with vulnerable plaque and complicated lesions in transplant recipients: new insight into cardiac allograft vasculopathy by optical coherence tomography. Eur Heart J 2013;34: 2610–7.

14. Ichibori Y, Ohtani T, Nakatani D, et al. Optical coherence tomography and intravascular ultrasound evaluation of cardiac allograft vasculopathy with and without intimal neovascularization. Eur Heart J Cardiovasc Imaging 2016;17:51–8.

15. Dong L, Maehara A, Nazif TM, et al. Optical coherence tomographic evaluation of transplant coronary artery vasculopathy with correlation to cellular rejection. Circ Cardiovasc Interv 2014;7: 199–206.

16. Tearney GJ, Yabushita H, Houser SL, et al. Quantification of macrophage content in atherosclerotic plaques by optical coherence tomography. Circulation 2003;107:113–9.

17. Matsuo Y, Cassar A, Li J, et al. Repeated episodes of thrombosis as a potential mechanism of plaque progression in cardiac allograft vasculopathy. Eur Heart J 2013;34:2905–15.

18. Thomas MR, Storey RF. The role of platelets in inflammation. Thromb Haemost 2015;114:449–58.

19. Modjeski KL, Morrell CN. Small cells, big effects: the role of platelets in transplant vasculopathy. J Thromb Thrombolysis 2014;37:17–23.

20. Abele S, Weyand M, Wollin M, et al. Clopidogrel reduces the development of transplant arteriosclerosis. J Thorac Cardiovasc Surg 2006; 131:1161–6.

21. Zhu J, Gao B. Simvastatin combined with aspirin increases the survival time of heart allograft by activating $CD4^{+}CD25^{+}$ Treg cells and enhancing vascular endothelial cell protection. Cardiovasc Pathol 2015;24:173–8.

22. Potena L, Masetti M, Sabatino M, et al. Interplay of coronary angiography and intravascular ultrasound in predicting long-term outcomes after heart transplantation. J Heart Lung Transplant 2015;34:1146–53.

KEY WORDS cardiac allograft vasculopathy, heart transplantation, intravascular imaging, optical coherence tomography, time-to-event analysis